Arch. Min. Sci. **68** (2023), 1, 103-123

Electronic version (in color) of this paper is available: http://mining.archives.pl

DOI: https://doi.org/10.24425/ams.2023.144320

JUN ZHANG[1], JIANNING LIU[1], YAJUN WANG[2*], GANG YANG[1], SHILIN HOU[1], YANJUN WANG[3], MANCHAO HE[1], JUN YANG[1]

STUDY ON PRESSURE RELIEF MECHANISM OF HYDRAULIC SUPPORT IN WORKING FACE UNDER DIRECTIONAL ROOF CRACK

When mining coal from the working face, the main roof withstands the overlying strata. The main roof's first weighting and periodic weighting may cause accidents, such as crushing the working face hydraulic supports. A mechanical model of the main roof was constructed, and the contributing factors of first and periodic weights on the main roof were examined in order to prevent such accidents. The thickness of the main roof was found as the most contributory factor to the main roof's stability. Therefore, a new directional roof crack (DRC) technique is proposed, which produces directional cracks in the main roof through directional blasting and makes part of it collapse in advance so as to reduce the thickness and relieve the first and periodic weighting. To verify the effectiveness of DRC, the mechanism of DRC was analysed. A mechanical model of the hydraulic support was constructed, and the DRC techniques were tested on-site. Field experiments with a complete set of monitoring schemes showed that, with DRC technology, the roof periodic weighting interval decreased by 35.36%, and the hydraulic support pressure decreased by 17.56%. The theoretical analysis was consistent with the measured results. Therefore, the DRC technology is feasible and effective to ensure mining safety at the working face.

Keywords: directional roof crack; pressure relief mechanism; main roof; hydraulic support pressure

1. Introduction

Coal, the primary energy source in China, has had a profound impact on the country's social and economic development. Globally, China is the world leader in coal production and consump-

[1] CHINA UNIVERSITY OF MINING & TECHNOLOGY (BEIJING), STATE KEY LABORATORY FOR GEOMECHANICS AND DEEP UNDERGROUND ENGINEERING, BEIJING 100083, CHINA
[2] SCHOOL OF CIVIL AND RESOURCE ENGINEERING, UNIVERSITY OF SCIENCE AND TECHNOLOGY BEIJING, BEIJING 100083, CHINA
[3] SHANXIYINFENG SCIENCE & TECHNOLOGY CO. LTD, TAIYUAN 030000, CHINA
* Corresponding author: wangyj@tongji.edu.cn

tion [1-4]. In the traditional longwall mining process, the roof's stability is crucial. It can be utilised to analyse the collapse of the rock layer while assessing its stability. One of the parameters that can estimate the stability of the roof is the index "g" [5]. Generally, the stability of one layer of rock in the roof is greater than that of the immediate roof, which is called the main roof. the immediate roof collapses behind the coal mine face. The length of the overhanging main roof keeps increasing with the increase of goaf space until it collapses. As the main roof withstands the overlying strata [6-8], the first and periodic weighting of the main roof leads to violent movement of the overburden with apparent dynamic loading and an increase of mining pressure. At the same time, the instability of the main roof causes a sudden pressure increase in the hydraulic support, leading to strong ground pressure disasters such as the crushing of hydraulic support and damage to working face equipment [9-13]. In coal mines with gas outbursts, roof instability can also lead to gas accidents, which often pose serious threats to the safety of coal mine production [14-16]. Therefore, in order to maintain mining pressure at the working face, optimise hydraulic supports, and ensure coal production safety, it is imperative to study the mechanical mechanism, contributing factors, and preventative methods of main roof weighting. In this study, the immediate roof is siltstone, the rock layer is grey, containing plant debris fossils, with horizontal and wavy bedding, the tensile strength is 0.39 Mpa, the rock layer is thin, the indirect roof is medium sandstone, grey-white, dominated by quartz, columnar structure, with large cross-bedding, the tensile strength is 0.58 Mpa, and the rock layer is thick. In contrast, medium sandstone is more difficult to collapse than siltstone, so it is studied as the main roof.

Scholars have made plentiful achievements studying the mechanical mechanism and contributory factors of main roof weighting. The key layer theory concluded that roof breakage is correlated with the physical property, thickness and location of the roof. Main roof weighting exerts additional pressure on the working face hydraulic supports [17]. Thickness, crack length and angle of the key layer are essential parameters determining the abutment pressure of the hydraulic support [18,19]. The greater the tensile strength of the roof layer, the longer the weighting interval [20]. The length of the main roof weighting interval can also increase with the increase in depth [21].

In addition to the contributory factors of main roof weighting, roof pressure relief methods were studied extensively. The stress state of the main roof can be obtained by theoretical and numerical analysis. With hydraulic fracturing, the pressure of the main roof is reduced to ensure safe production at the coal mine face [22]. To improve the effect of roof pressure relief, the horizontal tensile stress generated is utilised to promote fracture propagation during hydraulic fracturing [23]. By improving hydraulic fracturing technology, vertical fractures could be formed in the roof to further relieve the pressure [24]. Through laboratory test analysis, the main roof pressure can be relieved by deep hole blasting without causing rock burst accidents in the mining process [25].

Traditional deep hole blasting [26-28] and hydraulic fracturing [29-31] reduce roof pressure by making cracks in the roof. However, with deep-hole blasting, there is the risk of destroying the entire roof and even the roadway. With hydraulic fracturing, the direction and scope of the cracks are difficult to control, and the roof pressure relief is not ideal. Therefore, with the advancements in science and technology and mechanics theory [32-35], a more effective pressure relief method is required. To ensure the efficiency of pressure relief, the length and direction of roof cracks must be controlled. Therefore, an innovative approach based on directional roof crack (DRC) is proposed, which reduces the thickness of the main roof while not changing the mechanical properties so that both the mining pressure and the hydraulic support pressure could be reduced. The method was applied to a field test. By comparing relevant indicators, the overall pressure

of hydraulic support is reduced by using DRC technology compared with that without DRC technology, which can prove that DRC technology has a good pressure relief effect. This study provides a new way to reduce pressure and improve the safety and stability of hydraulic support.

2. Techniques and methods of DRC

DRC is implemented using directional blasting with shaped charges since the rock's compressive strength is significantly higher than its tensile strength [36]. The technology requires a combination of directional-shaped charge devices (DSCD) and conventional explosives. As shown in Fig. 1, the structure of DSCD is designed to be a tube with holes so that it could carry explosives into a borehole and release explosion energy through the holes.

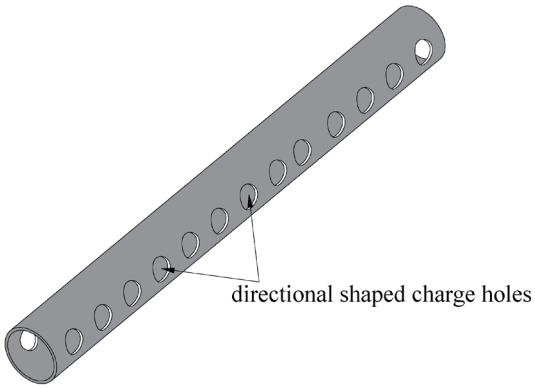

Fig. 1. The structure of DSCD

In conventional borehole blasting, the explosion energy diffuses in all directions, exerting a relatively uniform pressure on the surrounding rock mass, resulting in many random cracks around the borehole, as shown in Fig. 2a. With directional blasting, as shown in Fig. 2b, the explosion energy from conventional explosives loaded into the DSCD is released through the directional-shaped charge holes. Energy dissipation is avoided due to the directional-shaped charge holes and small compressibility of the DSCD. The explosion energy produces a reflected tensile stress perpendicular to the preset direction, and the crack expands continuously, causing the rock mass to crack along the preset direction.

The multihole blasting technique is adopted for DRC. A series of boreholes are drilled in the rock mass along the preset line with a certain interval. The number of explosives and the orientation of directional-shaped charge holes in the DSCD are then determined accordingly. With simultaneous explosions in multiple boreholes, the rock mass cracks along the directional-shaped charge holes while remaining intact in other directions.

A field test was carried out in an engineering project to observe the actual effect of DRC. In order to make the cracks in rock mass along the predetermined direction, the parameters of boreholes need to be designed. The main parameters are the diameter, length and spacing of the blasting hole. The diameter of the boreholes is determined by the diameter of the DSCD

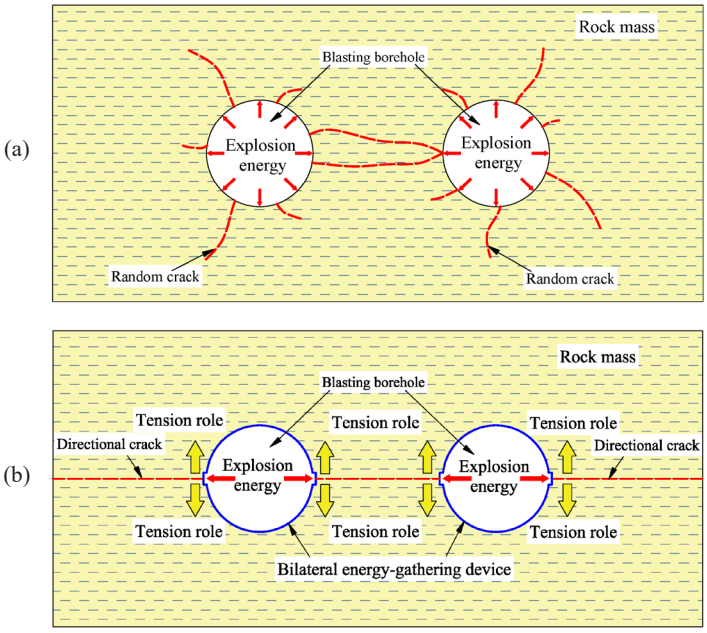

Fig. 2. Mechanical models of borehole blasting (a) Traditional borehole blasting, (b) Directional shaped charge blasting

and is normally 5-10 mm larger than the DRCD. The length of the boreholes is determined by the mining height. The spacing of the boreholes is determined by experience and field tests, usually 450-650 mm [37,38]. The boreholes were 2 m deep, 40 mm in diameter, and 500 mm apart from each other. The directional-shaped charge holes were arranged on the same plane of the tube axis. As shown in Fig. 3, a directional crack formed on the plane of the directional-shaped charge holes.

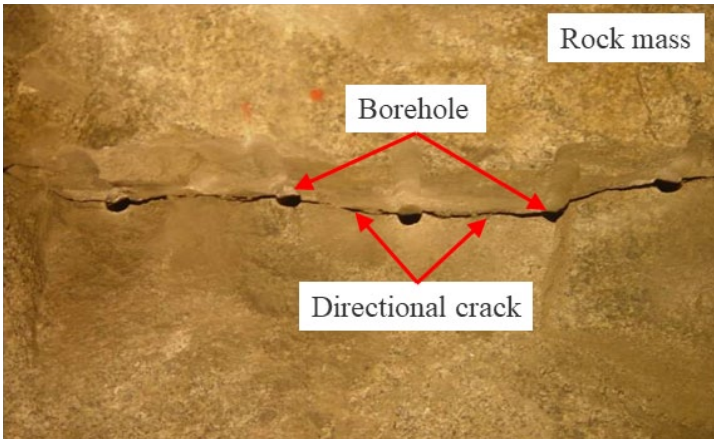

Fig. 3. Test results of DRC technology

3. Theoretical analysis of DRC

3.1. Mechanical analysis of the roof structure

As the direct cause of the mining pressure is the main roof weighting, DRC inevitably changes the law of mining pressure by altering the roof structure. Thus, a model, as shown in Fig. 4, is built to analyse the bearing characteristics of the main roof and the factors affecting its stability. The thickness of the coal seam, main roof and immediate roof are m (m), d (m) and h (m), respectively.

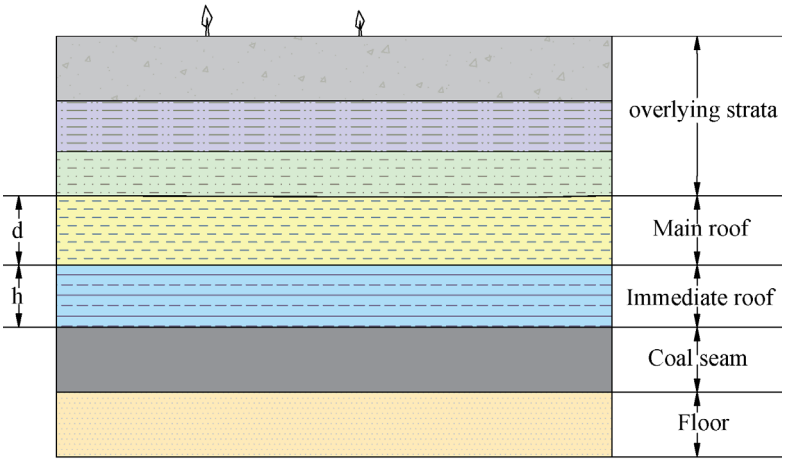

Fig. 4. Bearing characteristics of the main roof

Fig. 5a shows the mechanical model of the first weighting alongside the face of the coal mine, and the main roof is assumed to be a beam with both ends supported by the rock mass. According to elastic-plastic mechanics [39], the tensile stress and shear stress of any point in the beam are:

$$\begin{cases} \sigma_x = \dfrac{-6q}{d^3}x^2y + \dfrac{6q}{d^3}xy + \dfrac{4q}{d^3}y^3 - \left(\dfrac{qL^2}{d^3} + \dfrac{3q}{5d}\right)y \\ \tau_{xy} = \dfrac{6q}{d^3}xy^2 - \dfrac{3qL}{d^3}y^2 - \dfrac{3q}{2d}x + \dfrac{3qL}{4d} \end{cases} \tag{1}$$

Where L is the main roof weighting interval, m, q is the overburden load, MPa.

Assuming q = 0.4 MPa, d = 15 m, L = 50 m, the distribution of shear stress and tensile stress in the fixed-ends beam is shown in Fig. 6.

Fig. 6 shows that the maximum tensile stress appears at the upper and lower middle point of the beam. The tensile strength was less than the compressive strength of the rock mass, and the first crack appeared at both the upper ends and the lower middle point of the beam. In addition, the shear stress in the upper and lower middle points of the beam was zero, so the maximum

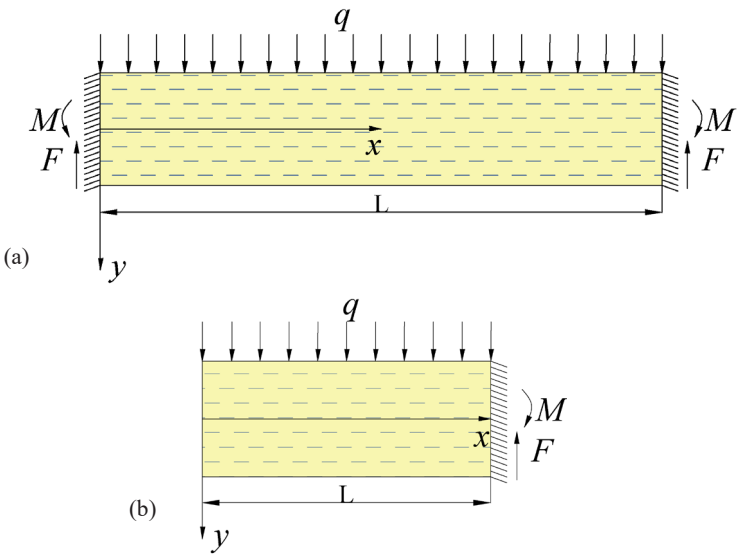

Fig. 5. Main roof mechanical model (a) a First weighting – fixed-ends beam, (b) Periodic weighting – cantilever beam

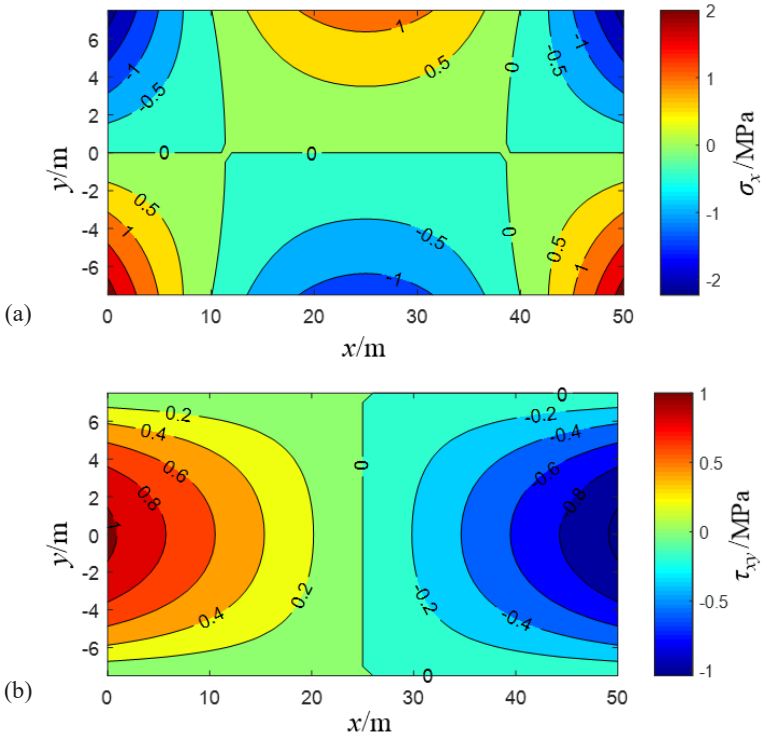

Fig. 6. Stress distribution in fixed-ends beam (a) Tensile stress distribution, (b) Shear stress distribution

principal stress there was equal to the tensile stress. The maximum tensile stress at the lower middle point ($L/2$, $d/2$) of the beam is:

$$\sigma_{\max} = \frac{q}{5} + \frac{qL^2}{4d^2}, \text{ MPa} \tag{2}$$

According to the failure criterion of maximum tensile stress, the condition for the main roof to collapse is:

$$\sigma_{\max} = \frac{\sigma_t}{n} \tag{3}$$

Where σ_t is the tensile strength of the main roof, MPa, n is the safety factor when the main roof collapses.

According to Equations (1), (2), and (3), the main roof first weighting interval L_f is:

$$L_f = 2d\sqrt{\frac{\sigma_t}{nq} - \frac{1}{5}}, \text{ m} \tag{4}$$

Fig. 5b shows the mechanical model of periodic weighting alongside the coal mine face, where the main roof is assumed to be a cantilever beam with a fixed end and a free end. According to elastic-plastic mechanics, the tensile stress and shear stress of any point in the cantilever beam is:

$$\begin{cases} \sigma_x = \dfrac{-6q}{d^3}x^2 y + \dfrac{4q}{d^3}y^3 - \dfrac{3q}{5d}y \\ \tau_{xy} = \dfrac{6q}{d^3}xy^2 - \dfrac{3q}{2d}x \end{cases} \tag{5}$$

Assuming $q = 0.4$ MPa, $d = 15$ m, $L = 50$ m, the distribution of shear stress and tensile stress in the cantilever beam is shown in Fig. 7.

Fig. 7 shows that the maximum tensile stress appears at the upper right end of the cantilever beam where the cracking first appears. The shear stress was zero at this position, so the maximum principal stress there was equal to the tensile stress. The maximum tensile stress at the upper right end (L, $-d/2$) of the beam is:

$$\sigma_{\max} = \frac{3qL^2}{d^2} - \frac{q}{5} \tag{6}$$

According to Equations (3), (5), and (6), the main roof periodic weighting interval L_p is:

$$L_p = d\sqrt{\frac{\sigma_t}{3nq} + \frac{1}{15}}, \text{ m} \tag{7}$$

According to Equation (4) and Equation (7), the main roof weighting interval is not only related to the tensile strength (σ_t), but also related to thickness of the main roof (d), the overlying strata load (q), and the thickness of the immediate roof (h). Moreover, the thickness of the main roof has the greatest influence on the weighting interval. As the main roof weighting interval

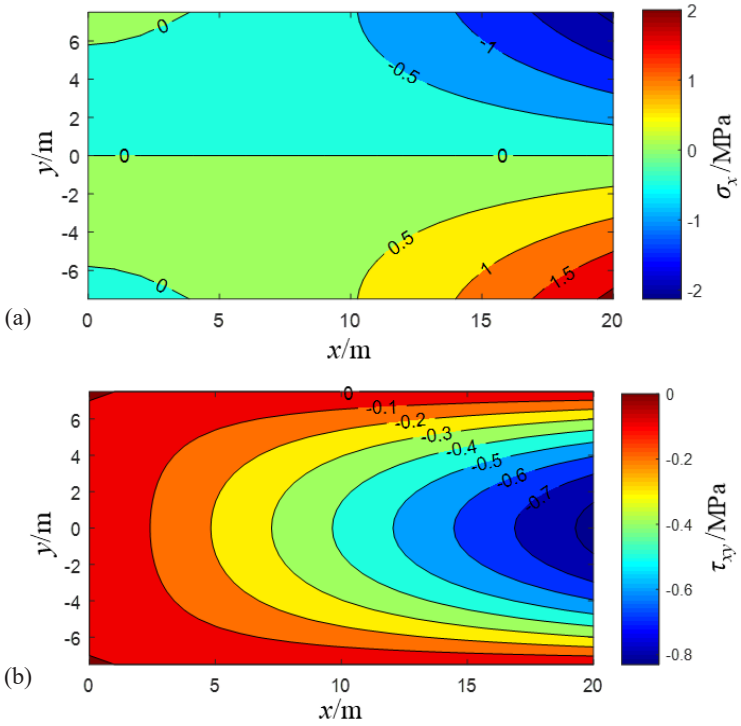

Fig. 7. Stress distribution in the cantilever beam (a) Tensile stress distribution, (b) Shear stress distribution

determines the magnitude of mining pressure behaviour, altering the largest contributory factor of the weighting interval will change the mining pressure behaviour to the greatest extent.

3.2. Mechanism of DRC technology

A comparison model, as shown in Fig. 8, is built to study the mechanism of DRC technology. The back of the hydraulic support is filled with gangue, the DRC technology cannot be used in the back of the hydraulic support, so DRC technology can only be used in the roadway near the goaf space. The DRC technology and the non-DRC technology are compared and analysed. In each case, two sections are selected for analysis, namely the section of the roadway and the section of the working face. The section of the roadway is convenient to analyse the mechanism of DRC on the roof structure, and the section of the working face is convenient to analyse the mechanism of DRC on the hydraulic support.

In the case of non-DRC technology, the roadway is damaged, the immediate roof collapses and the main roof sinks and breaks, Fig. 8a shows the structural features of the damaged roadway and the roof structure. The main roof undergoes periodic pressure under the load of overlying strata, the hydraulic support bears the force of the immediate roof itself and the force applying to the immediate roof. Fig. 8b shows the structural features of hydraulic support and roof structure.

In the case of DRC technology, the DRC technology is applied to create directional cracks

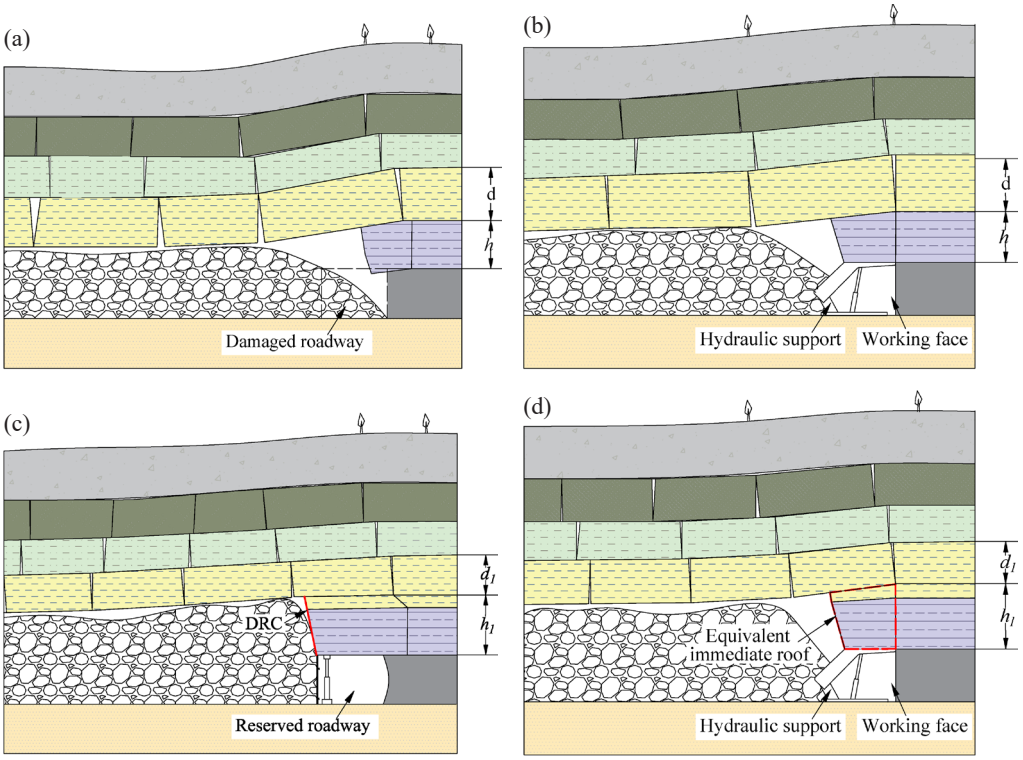

Fig. 8. Mechanism Model of DRC technology (a) The section of roadway with non-DRC technology, (b) The section of working face with non-DRC technology, (c) The section of roadway with DRC technology, (d) The section of working face with DRC technology

on the main roof over the roadway. The overhanging rock strata will collapse along the cracks. The structure of the main roof is changed as the vertical depth of the DRC exceeds the thickness of the immediate roof. Fig. 8c shows the structural features of the reserved roadway and the roof structure. The layer of the main roof within the vertical depth of the DRC breaks off with the collapse of the immediate roof. The broken layer of the main roof and the immediate roof can be assumed to be an equivalent immediate roof, thus, the thickness of the original main roof is reduced. The hydraulic support bears the force of the equivalent immediate roof itself and the force applying to the equivalent immediate roof, Fig. 8d shows the structural features of hydraulic support and roof structure.

After the application of DRC technology, define the thickness of the equivalent immediate roof is h_1 (m), then the thickness of the main roof is:

$$d_1 = h + d - h_1, \text{ m} \tag{8}$$

The main roof's thickness is the principal determinant of the weighting interval, as stated in Section 3.1, whilst the reduction of the first and periodic weighting intervals affects the pressure strength of the working pressure of the hydraulic supports at the working face. Therefore, the DRC technology is used to relieve the pressure of the hydraulic support.

3.3. Effect of DRC on hydraulic support pressure

The DRC alters the structure of the roof structure and affects the main roof weighting interval. Meanwhile, the stress state of the hydraulic support is also altered. Take periodic weighting as an example, when the working face undergoes periodic pressure, the hydraulic support bears the maximum pressure when it is located directly below the main roof breaking position, and the mechanical characteristics of the hydraulic support can be plotted in Fig. 9.

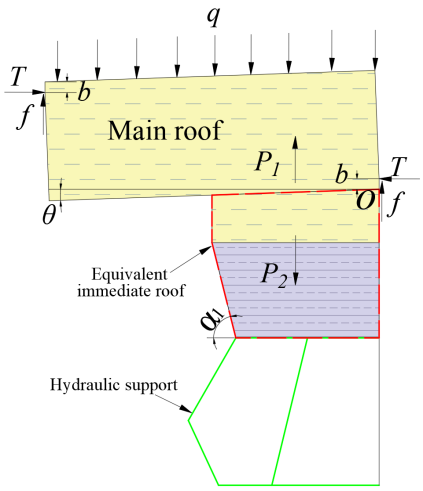

Fig. 9. Pressure characteristics of hydraulic support with DRC technology

Considering the hinged relationship between the rock blocks after the main roof is broken [17], the position of horizontal thrust and friction force between rock blocks can be calculated as:

$$b = \frac{1}{4}\left(h - L_P \sin\theta\right), \text{ m} \tag{9}$$

Where θ is the angle of rock rotation sinking, the angle is small when the main roof is broken, usually $\theta = 3°$.

To keep the main roof stable, let $\Sigma F_y = 0$ and $\Sigma M_o = 0$, then,

$$2f + P_1 = qL_p c \tag{10}$$

$$\frac{1}{2}cqL_p \cos\theta\left(\frac{1}{2}L_p \cos\theta + d_1 \sin\theta\right) = f\left(L_p \cos\theta + d_1 \sin\theta\right) +$$

$$+T\left(d_1 \cos\theta - L_p \sin\theta - 2b\right) + P_1\left(\frac{a}{2} + \frac{h}{2}\cot\alpha_1\right) \tag{11}$$

Where T is the horizontal thrust between the rocks, kN, P_1 is the force of the immediate roof on the main roof, kN, α_1 is broken angle of the immediate roof, f is the friction force, kN.

The relationship between f and T is usually:

$$f = \mu T \tag{12}$$

Where μ is the friction factor between rock blocks, according to a large number of experiments, usually $\mu = 0.3$.

According to Equations (9), (10), (11), and (12), P_1 can be calculated as:

$$P_1 = \frac{cqL_p\left[\begin{array}{l}\mu\left(L_p\cos\theta + d_1\sin\theta\right) + d_1\cos\theta - L_p\sin\theta \\ -\frac{1}{2}\left(h - L_p\sin\theta\right) - \mu\cos\theta\left(\frac{1}{2}L_p\cos\theta + d_1\sin\theta\right)\end{array}\right]}{\begin{array}{l}\mu(L_p\cos\theta + d_1\sin\theta) + d_1\cos\theta - L_p\sin\theta \\ -\frac{1}{2}\left(h - L_p\sin\theta\right) - \mu\left(a + \cot\alpha_1\right)\end{array}} \tag{13}$$

The weight of the equivalent immediate roof P_2 is completely supported by the hydraulic support. P_2 can be expressed as:

$$P_1 = c\gamma_1\left(h_1 - h - \frac{h}{2}\cot\alpha - \frac{a}{2}\right)\left(a + h\cot\alpha\right) + ch\gamma_2\left(a + \frac{h}{2}\cot\alpha\right), \text{ kN} \tag{14}$$

Where γ_1 and γ_2 are the bulk density of main roof and immediate roof, respectively, N/m^3, c is the average distance between adjacent hydraulic supports, m, a is the roof beam length of the hydraulic support, m.

The hydraulic support pressure is the sum of the gravity of the immediate roof and the force of the immediate roof on the main roof, according to Equations (13) and (14), the working pressure P of the hydraulic support is:

$$P = P_1 + P_2 = \frac{cqL_p\left[\begin{array}{l}\mu\left(L_p\cos\theta + d_1\sin\theta\right) + d_1\cos\theta - L_p\sin\theta \\ -\frac{1}{2}\left(h - L_p\sin\theta\right) - \mu\cos\theta\left(\frac{1}{2}L_p\cos\theta + d_1\sin\theta\right)\end{array}\right]}{\begin{array}{l}\mu\left(L_p\cos\theta + d_1\sin\theta\right) + d_1\cos\theta - L_p\sin\theta \\ -\frac{1}{2}\left(h - L_p\sin\theta\right) - \mu\left(a + \cot\alpha_1\right)\end{array}}$$
$$+c\gamma_1\left(h_1 - h - \frac{h}{2}\cot\alpha_1 - \frac{a}{2}\right)\left(a + h\cot\alpha_1\right) + ch\gamma_2\left(a + \frac{h}{2}\cot\alpha_1\right), \text{ kN} \tag{15}$$

3.4. Vertical depth and angle of the DRC

Both the vertical depth and angle affect the effectiveness of DRC. On the one hand, the thickness of the main roof has the greatest influence on the mining pressure behaviour, so the vertical depth of the DRC should exceed the immediate roof. On the other hand, the DRC needs to have

a certain angle so that the roof could collapse along the crack. As shown in Fig. 10, defined α_2 as the angle of the DRC and $h_c \cos\alpha_2$ as the vertical depth of the DRC, then:

$$h_c \cos\alpha_2 \geq h \tag{16}$$

Where h_c is the depth of the DRC, m.

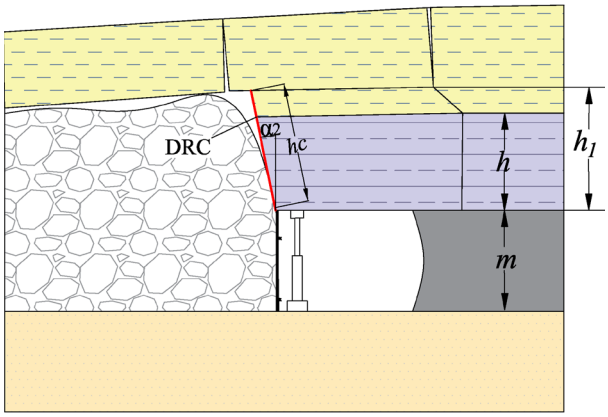

Fig. 10. Vertical depth and angle of the DRC

Theoretically, the volume of the complete rock mass expands after the collapse [40]. If the roof strata are full of goaf after collapse, the height of DRC is good and the effect is the best, namely:

$$h_c \cos\alpha_2 \leq \frac{m}{k-1} \tag{17}$$

Where k is the fracture swelling coefficient of rock mass.

The thickness of the equivalent immediate roof is:

$$h_1 = h_c \cos\alpha_2 \tag{18}$$

4. Field testing

4.1. Testing location and parameters

To verify the effectiveness of DRC, the Ningtiaota coal mine, located in Shenmu County, Yulin City, Shannxi Province, China, as shown in Fig. 11, was selected as the testing site. The mined coal seam is the N0.2^{-2} with an average thickness of 4.11 m. The dip angle of the coal seam is nearly horizontal. Two adjacent working faces are selected for the test, one is S1201-I and the other is S1201-II, as shown in Fig. 12. The DRC technique was applied in the ventilation roadway of working face S1201-II during mining while not applied during face mining of S1201-I. Considering the geological data, the geological parameters of the coal mine face can

be concluded that $d = 18.60$ m, $h = 2.20$ m and $m = 4.11$ m, the parameters of hydraulic supports can be concluded that $c = 1.75$ m and $a = 5.45$ m, according to laboratory tests, other parameters can be concluded that $q = 0.45$ MPa, $\sigma_t = 0.58$ MPa, $k = 1.43$, $\alpha_1 = 60°$, $\gamma_1 = 2.7\times10^3$ N/m^3 and $\gamma_2 = 2.5\times10^3$ N/m^3.

Fig. 11. The position of coal mine

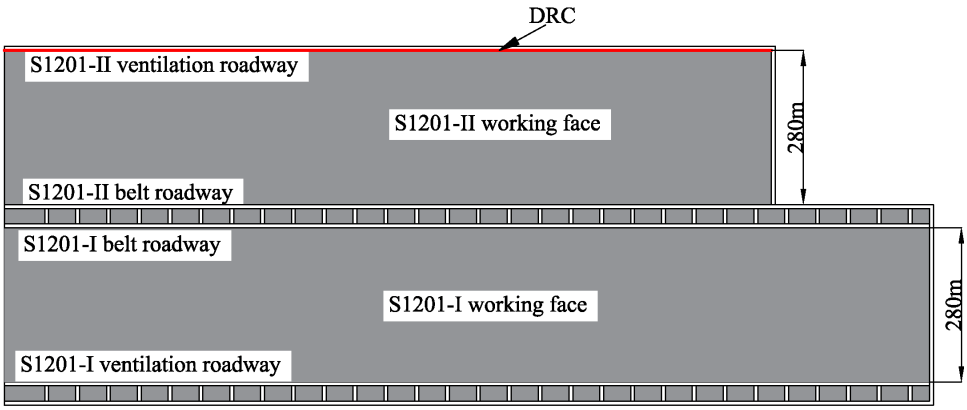

Fig. 12. Situation of the test working face

According to Section 3.5, 2.20 m $\le h_c \cos\alpha_2 \le$ 9.55 m. Based on a previous study [41], the DRC angle α_2 is usually around 10° and 20°. The geological and construction conditions of the test site are considered comprehensively, the DRC angle is set to $\alpha_2 = 10°$. Therefore, 2.23 m $\le h_c \le$ 9.70 m. According to the site construction conditions, DRC parameters were set as $h_c = 9$ m and $\alpha_2 = 10°$ to achieve the best pressure relief effect. According to Equation (18), $h_1 = 8.86$ m.

The DRC design of the ventilation roadway at the S1201-II coal mine face is shown in Fig. 13a. To protect the safety of the roadway, we use a longer anchor cable than the DRC vertical length to support the roadway and reduce the damage of the blasting to the roadway. The explosives used in DRC are emulsion explosives. Each roll of explosive has a weight of 200 g, a length of 200 mm and a diameter of 32 mm. The length of each DCSD is 1500 mm, with a diameter of 42 mm. In order to put DSCD into the boreholes, the diameter of the boreholes is designed to be 50 mm. Five DSCDs are placed in each borehole, and the charging structure of "4+4+3+3+2" is adopted in the borehole. The length of the sealing borehole is 1.5 m. One detonator is placed in each DCSD. The spacing between adjacent boreholes is 600 mm. The charging parameter design of DRC is shown in Fig. 13b. In order to determine the effect of the application of DRC, we used an in-situ monitoring method to observe the crack. After using DRC technology, a directional crack appeared between adjacent holes in the roof, as shown in Fig. 14a. Meanwhile, a borehole peeping device was used to monitor the development of cracks in the borehole. Fig. 14b is the device diagram of borehole peeping, and Fig. 14c is the development of cracks in the borehole. There are two clearly visible balance cracks in the borehole that run almost the entire length of the borehole, which demonstrates the excellent effect of DRC.

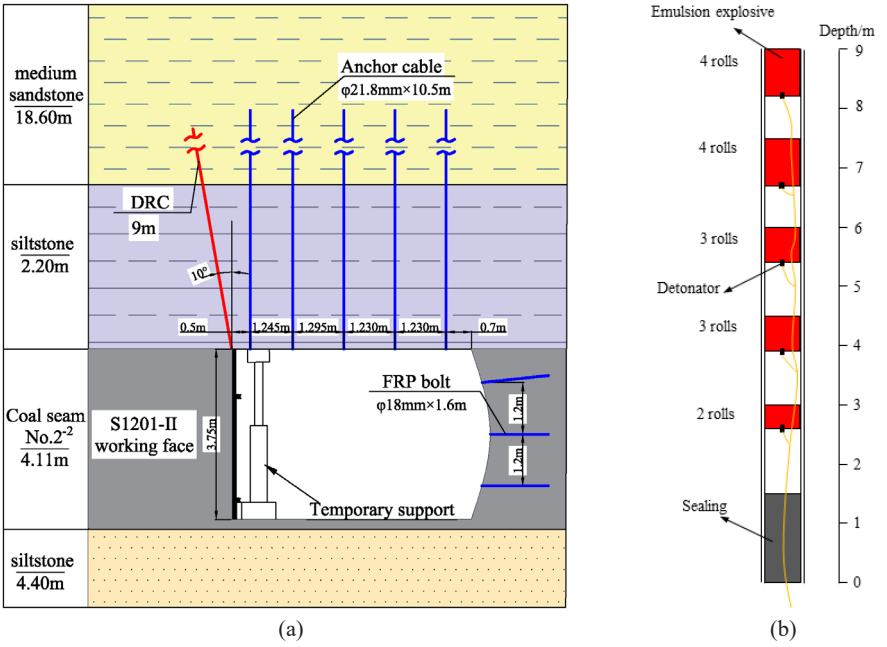

Fig. 13. Working face S1201-II ventilation roadway and DRC design (a) DRC design of ventilation roadway at S1201-II working face, (b) charging parameter design of DRC

To prove the validity of DRC on pressure relief of hydraulic support, pressure sensors were mounted on every tenth of the 160 hydraulic supports at the working face. The pressure of the hydraulic supports was recorded. The number and location of the pressure sensors on the two working faces are consistent. The detailed installation position of the pressure sensors is shown

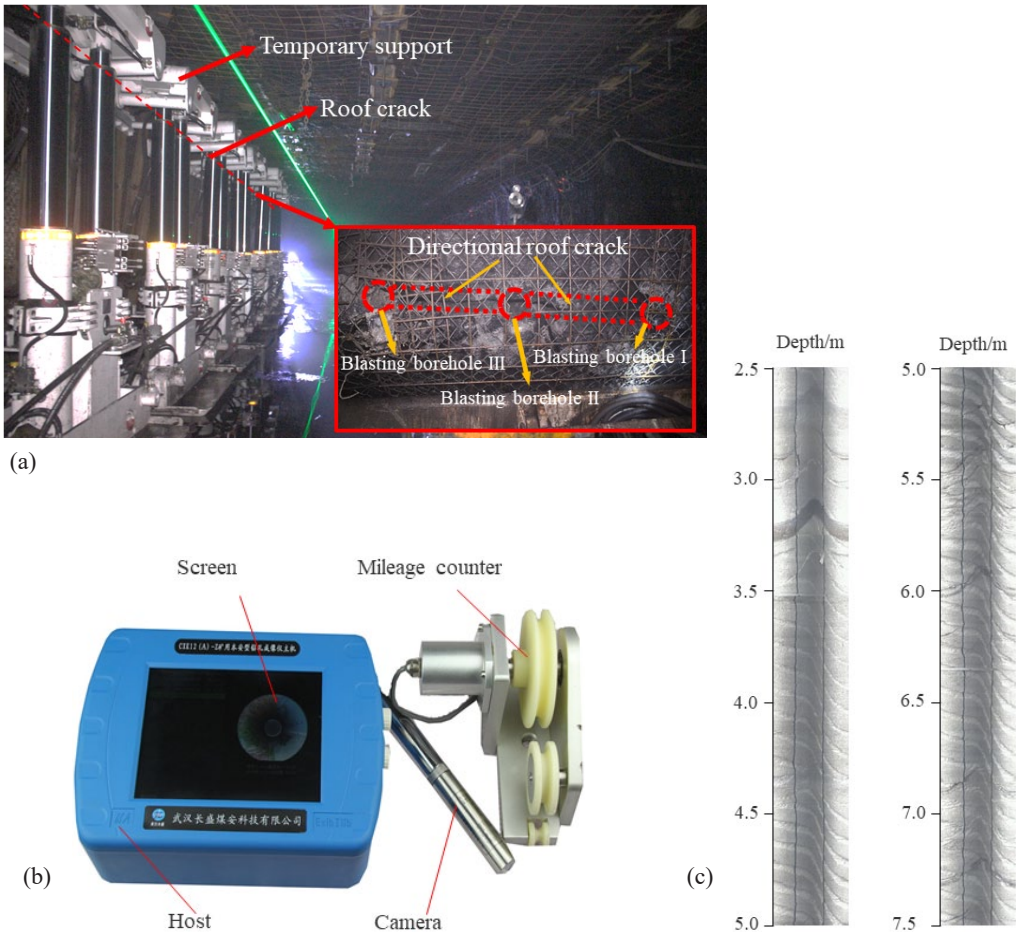

Fig. 14. In-situ monitoring of the DRC effect (a) Renderings of DRC site construction, (b) device diagram of borehole peeping, (c) development of cracks in the borehole

in Fig. 15. The effect of DRC is analysed by observing the mining pressure behaviour at the two working faces and the pressure of the hydraulic supports.

4.2. Results and analysis

Based on the above research, the theoretical analysis results of the mining pressure behaviour of working faces S1201-I and S1202-II were acquired. Taking the periodic weighting as an example, according to Equation (7), the working face S1201-I periodic weighting interval L_p = 13.10 m, working face S1201-II periodic weighting interval L_p' = 8.41 m. According to Equation (15), the hydraulic support pressure at working face S1201-I during periodic weighting P = 10352 kN, and the hydraulic support pressure at working face S1201-II during periodic weighting P' = 8567 kN.

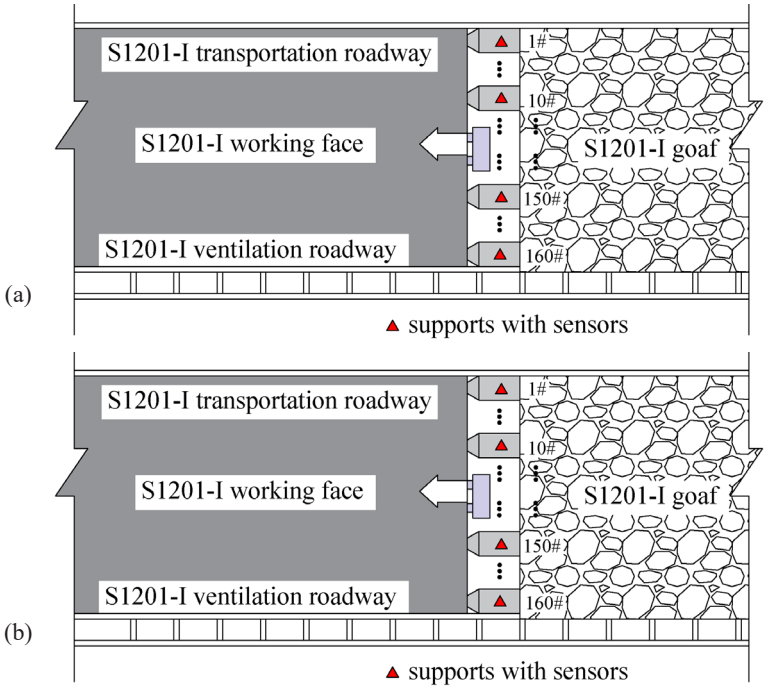

Fig. 15. The detailed layout of the pressure sensors (a) working face S1201-I pressure sensors layout, (b) working face S1201-II pressure sensors layout

To verify the effectiveness of DRC technology and the accuracy of the theoretical analysis, the working pressure of the hydraulic supports is recorded by the pressure sensors of the coal mine face. The geological conditions of the site and other factors affecting the mining pressure behaviour with the advance of the coal mine face, such as faults, trap columns, and other geological formations, were also considered. The hydraulic support pressure within 60 m along the advance of the two working faces was selected for the analysis. The monitoring data of hydraulic support is shown in Fig. 16 and Table 1. The average hydraulic support pressure at working face S1201-I during periodic weighting is 10013 kN, and the average interval of periodic weighting at working face S1201-Iis 13.80 m. For the working face S1201-II that adopted the DRC approach, the average hydraulic support pressure during periodic weighting is 8255 kN, and the average interval of periodic weighting is 8.92 m. The difference between the field measurement data and theoretical analysis results is negligible, which proves the effectiveness of DRC technology and the accuracy of theoretical analysis.

TABLE 1

The periodic weighting average length and hydraulic support average pressure of the working face

Working face	Periodic weighting average length /m	Hydraulic support average pressure /KN
S1201-I	13.80	10013
S1201-II	8.92	8255

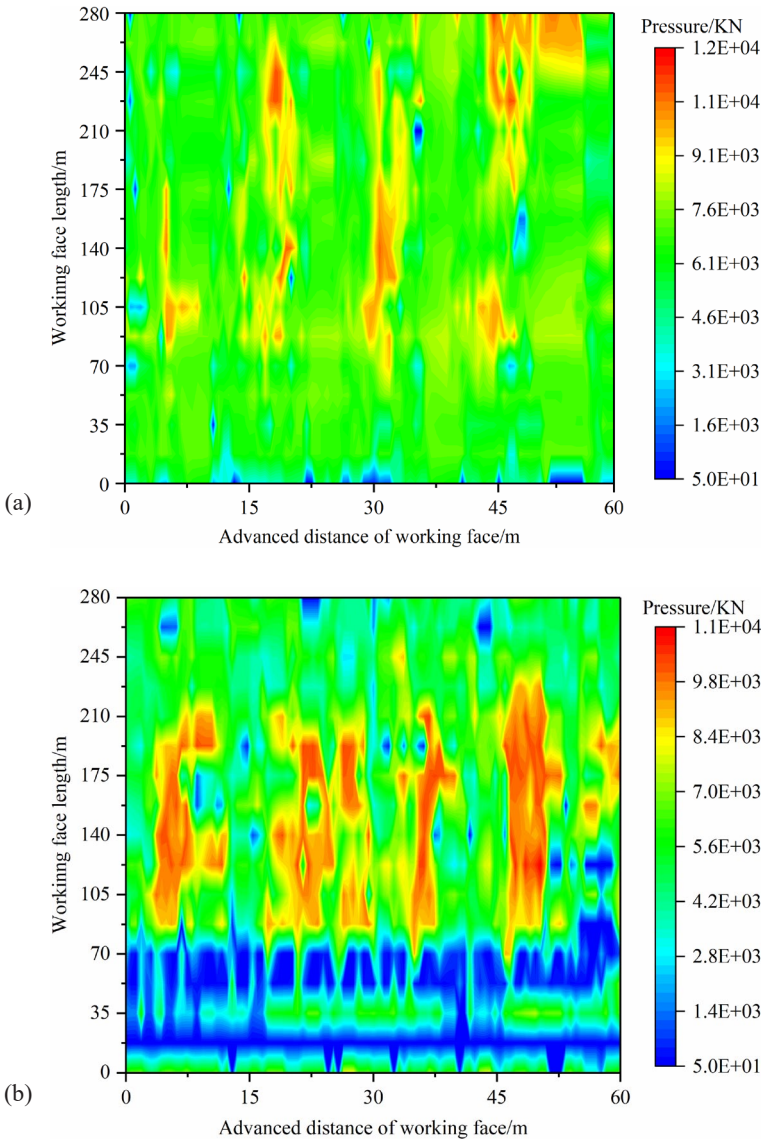

Fig. 16. Monitoring data from the working face (a) working face S1201-I hydraulic support pressure, (b) working face S1201-II hydraulic support pressure

Theoretical analysis and field measurement data show that after the application of the DRC technique, the working face periodic weighting interval decreases by 35.36% and the average hydraulic support pressure during periodic weighting decreases by 17.56%. Therefore, DRC is an effective way to reduce mining pressure and hydraulic support pressure.

5. Discussion

Theoretical analysis and field data show that the DRC technology is effective for pressure relief at the working face. DRC reduced the thickness of the main roof, which leads to a reduction of the periodic weighting interval and hydraulic support pressure. DRC technology is also adopted to reduce the risk of hydraulic support damage due to excessive pressure and to ensure safe production. However, the conclusions are drawn under certain assumptions. Firstly, there must be a main roof structure because the main roof structure withstands the overlying strata. The weighting of the main roof will cause a dramatic increase in hydraulic support pressure that leads to damage to the hydraulic supports. For working faces with broken roof rocks, there may not necessarily be a main roof structure, so the conclusions in this study may not be applicable. Secondly, the thickness of the roof needs to fall within certain limits. According to Section 3.4, the vertical depth of the DRC needs to exceed the thickness of the immediate roof, and part of the main roof needs to collapse. This will not work if the main roof is too thin or the immediate roof is too thick, as the blasting boreholes may exceed the main roof or not reach it, resulting in total or no main roof collapse. Finally, part of the main roof collapsed after adopting the DRC technology, yet due to the extensive length of the coal mine face, the length of the collapsed main roof is unclear. The scope of the influence of working face pressure relief is currently unclear, but according to the current on-site measured data, pressure relief on the entire working face is effective.

In this study, it should be noted that monitoring the pressure of the hydraulic support also helps to improve the safety level of the working face. This is because the pressure of the hydraulic support can effectively reflect the interaction between the hydraulic support and the rock stratum [42-44], which can be used to reflect the caving behaviour of the main roof. By studying the pressure data, the safety and efficiency of the mining face can be improved.

The geological conditions in this study are relatively simple. The coal seam is shallow and nearly horizontal, the test site strata are stable, and the thickness of the overlying strata meets the theoretical analysis conditions. Although the current method has been successfully implemented and verified, the data is small and not representative. More experiments should be conducted under different geological conditions and different mining parameters. More extensive test data should be recorded to verify the effectiveness and feasibility of this method.

6. Conclusions

In this study, the pressure relief mechanism of hydraulic support in the working face under DRC is analysed. The structure of the main roof is altered by DRC so that both the mining pressure and hydraulic support pressure are reduced. With the mechanic's calculation model of the main roof, it is found that the thickness of the main roof has the largest contributory factor to the hydraulic support pressure. Therefore, the thickness of the main roof was altered by the DRC technique. The optimal vertical depth of DRC was determined according to the distance between the main roof and the roadway roof and the rock mass bulking factor. The stress model of the working face hydraulic supports was built to discuss the influence of the DRC technique on the hydraulic support pressure. DRC technique reduced the thickness of the main roof, thus reducing the periodic weighting interval and the working pressure of the hydraulic supports, which ensured the safe production of the coal mine face.

The use of DRC technology can effectively reduce the pressure of hydraulic support and reduce the mine pressure behaviour of the working face so that the hydraulic support can work under lower pressures. Through the pressure value of the hydraulic support, we can know the collapse state of the main roof. When the roof is pressed periodically, the pressure of the hydraulic support increases. When the roof is not pressed periodically, the pressure of the hydraulic support is kept at a lower value. Studying the pressure value of the hydraulic support is helping to improve the safety and efficiency of the working face.

Field test data shows that the theoretical analysis is consistent with the measured results with negligible error. The hydraulic support pressure at the working face is reduced, and the pressure relief is satisfactory. This proves the feasibility and effectiveness of DRC technology.

Acknowledgments

This work is supported by the State Key Laboratory for Geomechanics and Deep Underground Engineering Shanxi Yinfeng Branch Center Foundation (No. YFKT-202002), the Institute for Deep Underground Science and Engineering, China University of Mining & Technology, Beijing (No. XD2021023), China Scholarship Council (202206430047) and the National Natural Science Foundation of China (Nos. 51904207, 52074164, 42077267), which are gratefully acknowledged.

Conflict of Interest

The authors declare no competing interests.

References

[1] H. He, L.M. Dou, S.Y. Gong, J. He, Y.L Zheng, Microseismic and Electromagnetic Coupling Method for Coal Bump Risk Assessment Based on Dynamic Static Energy Principles. Safety. Sci. **114**, 30-39 (2019). DOI: https://doi.org/10.1016/j.ssci.2018.12.025

[2] Z. He, Q. Wu, L.J. Wen, G. Fu, A Process Mining Approach to Improve Emergency Rescue Processes of Fatal Gas Explosion Accidents in Chinese Coal Mines. Safety. Sci. **111**, 154-166 (2019). DOI: https://doi.org/10.1016/j.ssci.2018.07.006

[3] J.H. Wang, Development and Prospect on Fully Mechanized Mining in Chinese Coal Mines. Int. J. Coal. Sci. Techno. **1**, 253-260 (2014). DOI: https://doi.org/10.1007/s40789-014-0017-2

[4] W. Yin, J.Q. Wang, X.M. Bai, W.J. Sun, Z.Y. Zhou, Strata Behavior and Control Strategy of Backfilling Collaborate with Caving Fully-mechanized Mining. Open. Geosci. **12** (1), 703-717 (2020). DOI: https://doi.org/10.1515/geo-2020-0168

[5] K. Skrzypkowski, W. Korzeniowski, T.N. Duc, Choice of powered roof support FAZOS-15/31-POz for Vang Danh hard coal mine. Inzh. Miner. **2** (2), (2022). DOI: https://doi.org/10.29227/IM-2019-02-71

[6] H.J. Jiang, S.G. Cao, Y. Zhang, C. Wang, Analytical Solutions of Hard Roof's Bending Moment, Deflection and Energy Under the Front Abutment Pressure Before Periodic Weighting. Int. J. Min. Sci. Techno. **26** (1), 175-181 (2016). DOI: https://doi.org/10.1016/j.ijmst.2015.11.027

[7] B. Zhang, S.G. Cao, Study on First Caving Fracture Mechanism of Overlying Roof Rock in Steep Thick Coal Seam. Int. J. Min. Sci. Techno. **25** (1), 133-138 (2015). DOI: https://doi.org/10.1016/j.ijmst.2014.11.013

[8] Q.L. Zou, H. Liu, Y.J. Zhang, Q.M. Li, J.W. Fu, Q.T. Hu, Rationality Evaluation of Production Deployment of Outburst-prone Coal Mines: A Case Study of Nantong Coal Mine in Chongqing. Safety. Sci. **122**, 104515 (2020). DOI: https://doi.org/10.1016/j.ssci.2019.104515

[9] X.W. Feng, N. Zhang, F. Xue, Z.Z. Xie, Practices, Experience, and Lessons Learned Based on Field Observations of Support Failures in Some Chinese Coal Mines. Int. J. Rock. Mech. Min. Sci. **123**, 104097 (2019). DOI: https://doi.org/10.1016/j.ijrmms.2019.104097

[10] Y.J. Wang, Q. Wang, X.C. Tian, H.S. Wang, J. Yang, M.C. He, Stress and deformation evolution characteristics of gob-side entry retained by roof cutting and pressure relief. Tunn. Undergr. Sp. Tech. **123**, 104419 (2022). DOI: https://doi.org/10.1016/j.tust.2022.104419

[11] D.M. Pappas, C. Mark, Roof and Rib Fall Incident Trends: A 10-year Profile. Trans. Soc. Min. Metal. Explor. **330**, 462-478 (2012).

[12] M.X. Wang, T. Zhang, M.R. Xie, B. Zhang, M.Q. Jia, Analysis of National Coal-mining Accident Data In China, 2001-2008. Public. Health. Rep. **126**, 270-275 (2011).

[13] D.F. Yang, Y.J. Zhang, Z.H. Chen, Analysis on Catastrophe Theory During First Weighting Sliding Instability and Support Crushing of Main Roof with Large Mining Height in Shallow Coal Seam. Appl. Sci. **10** (16), 5408 (2020). DOI: https://doi.org/10.3390/app10165408

[14] P. Konicek, J. Schreiber, Heavy Rockbursts Due to Longwall Mining Near Protective Pillars: A Case Study. Int. J. Min. Sci. Techno. **28** (5), 799-805 (2018). DOI: https://doi.org/10.1016/j.ijmst.2018.08.010

[15] A. Shadrin, Y. Diyuk, Geophysical Criterion of Pre-outburst Coal Outsqueezing From the Face Space Into the Working. Int. J. Min. Sci. Techno. **29** (3), 499-506 (2019). DOI: https://doi.org/10.1016/j.ijmst.2018.11.001

[16] W.T. Song, J.W. Cheng, W.H. Wang, Y. Qin, Z. Wang, M. Borowski, Y. Wang, P. Tukkaraja, Underground Mine Gas Explosion Accidents and Prevention Techniques – An overview. Arch. Min. Sci. **66** (2), 297-312 (2021). DOI: https://doi.org/10.24425/ams.2021.137463

[17] M.G. Qian, X.X. Miao, J.L. Xu, Theoretical Study of Key Stratum in Ground Control. Journal of China Coal Society **21**, 225-230 (1996).

[18] S.K. Das, Observations and Classification of Roof Strata Behaviour Over Longwall Coal Mining Panels in India. Int. J. Rock. Mech. Min. Sci. **37** (4), 585-597 (2000). DOI: https://doi.org/10.1016/S1365-1609(99)00123-9

[19] H. Yavuz, An Estimation Method for Cover Pressure Re-establishment Distance and Pressure Distribution in the Goaf of Longwall Coal Mines. Int. J. Rock. Mech. Min. Sci. **41** (2), 193-205 (2004). DOI: https://doi.org/10.1016/S1365-1609(03)00082-0

[20] M. Shabanimashcool, L. Jing, C.C. Li, Discontinuous Modelling of Stratum Cave-in in a Longwall Coal Mine in the Arctic Area. Geotech. Geol. Eng. **32**, 1239-1252 (2014). DOI: https://doi.org/10.1007/s10706-014-9795-y

[21] Q.S. Bai, S.H. Tu, F.T. Wang, C. Zhang, Field and Numerical Investigations of Gateroad System Failure Induced by Hard Roofs in a Longwall Top Coal Caving Face. Int. J. Coal Geol. **173**, 176-199 (2017). DOI: https://doi.org/10.1016/j.coal.2017.02.015

[22] H.F. Duan, L.J. Zhao, Prevention Technology for Strong Mine Pressure Disaster in the Hard-Roof Large-Mining-Height Working Face. Shock. Vib. **2020**, 8846624 (2020). DOI: https://doi.org/10.1155/2020/8846624

[23] J.W. Liu, C.Y. Liu, Q.L. Yao, G.Y. Si, The Position of Hydraulic Fracturing to Initiate Vertical Fractures in Hard Hanging Roof for Stress Relief. Int. J. Rock. Mech. Min. Sci. **132**, 104328 (2020). DOI: https://doi.org/10.1016/j.ijrmms.2020.104328

[24] H. He, L.M. Dou, J. Fan, T.T. Du, X.L. Sun, Deep-hole Directional Fracturing of Thick Hard Roof for Rockburst Prevention. Tunn. Undergr. Sp. Tech. **32**, 34-43 (2012). DOI: https://doi.org/10.1016/j.tust.2012.05.002

[25] P. Konicek, K. Soucek, L. Stas, R. Singh, Long-hole Destress Blasting for Rockburst Control During Deep Underground Coal Mining. Int. J. Rock. Mech. Min. Sci. **61**, 141-153 (2013). DOI: https://doi.org/10.1016/j.ijrmms.2013.02.001

[26] J.S. Guo, L.Q. Ma, Y. Wang, F.T. Wang, Hanging Wall Pressure Relief Mechanism of Horizontal Section Top-Coal Caving Face and Its Application – A Case Study of the Urumqi Coalfield, China. Energies. **10** (9), 1371 (2017). DOI: https://doi.org/10.3390/en10091371

[27] S.Q. He, D.Z. Song, Z.L. Li, X.Q. He, J.Q. Chen, T.P. Zhong, Q. Lou, Mechanism and Prevention of Rockburst in Steeply Inclined and Extremely Thick Coal Seams for Fully Mechanized Top-Coal Caving Mining and Under Gob Filling Conditions. Energies. **13** (6), 1362 (2020). DOI: https://doi.org/10.3390/en13061362

[28] J.X. Yang, C.Y. Liu, B. Yu, Application of Confined Blasting in Water-Filled Deep Holes to Control Strong Rock Pressure in Hard Rock Mines. Energies. **10** (11), 1874 (2017). DOI: https://doi.org/10.3390/en10111874

[29] Q.Y. Cheng, B.X. Huang, L.Y. Shao, X.L. Zhao, S.L Chen, H.Z. Li, C.W. Wang, Combination of Pre-Pulse and Constant Pumping Rate Hydraulic Fracturing for Weakening Hard Coal and Rock Mass. Energies. **13** (21), 5534 (2020). DOI: https://doi.org/10.3390/en13215534

[30] Z.J. Feng, W.B. Guo, F.Y. Xu, D.M. Yang, W.Q. Yang, Control Technology of Surface Movement Scope with Directional Hydraulic Fracturing Technology in Longwall Mining: A Case Study. Energies. **12** (18), 3480 (2019). DOI: https://doi.org/10.3390/en12183480

[31] D. Liu, Y.B. Wang, X.M. Ni, C.Q. Tao, J.J. Fan, X. Wu, S.H. Zhao, Classification of Coal Structure Combinations and Their Influence on Hydraulic Fracturing: A Case Study From the Qinshui Basin, China. Energies. **13** (17), 4559 (2020). DOI: https://doi.org/10.3390/en13174559

[32] M. Alber, R. Bischoff, M. Bischoff, T. Meier, Rock Mechanical Investigations of Seismic Events in a Deep Longwall Coal Mine. Int. J. Rock. Mech. Min. Sci. **46** (2), 408-420 (2009). DOI: https://doi.org/10.1016/j.ijrmms.2008.07.014

[33] W. Cai, L.M. Dou, M. Zhang, W.Z. Cao, J.Q. Shi, L.F. Feng, A Fuzzy Comprehensive Evaluation Methodology for Rock Burst Forecasting Using Microseismic Monitoring. Tunn. Undergr. Sp. Tech. **80**, 232-245 (2018). DOI: https://doi.org/10.1016/j.tust.2018.06.029

[34] L.M. Dou, X.Q. He, H. He, J. He, J. Fan, Spatial Structure Evolution of Overlying Strata and Inducing Mechanism of Rockburst in Coal Mine. T. Nonferr. Metal. Soc. **24** (4), 1255-1261 (2014). DOI: https://doi.org/10.1016/S1003-6326(14)63187-3

[35] S. Yang, J. Wang, X.H. Li, J.G. Ning, P.Q. Qiu, In Situ Investigations Into Mining-induced Hard Main Roof Fracture in Longwall Mining: A Case Study. Eng. Fail. Anal. **106**, 104188 (2019). DOI: https://doi.org/10.1016/j.engfailanal.2019.104188

[36] M.C. He, X.Y. Zhang, S. Zhao, Directional Destress with Tension Blasting in Coal Mines. Procedia. Engineer. **191**, 89-97 (2017). DOI: https://doi.org/10.1016/j.proeng.2017.05.158

[37] J. Yang, B.H. Liu, W.H. Bian, K.K. Chen, H.Y. Wang, C. Cao, Application Cumulative Tensile Explosions for Roof Cutting in Chinese Underground Coal Mines. Arch. Min. Sci. **66** (3), 421-435 (2021). DOI: https://doi.org/10.24425/ams.2021.138598

[38] X.Y. Zhang, R.Y.S. Pak, Y.B. Gao, C.K. Liu, C. Zhang, J. Yang, M.C. He, Field Experiment on Directional Roof Presplitting for Pressure Relief of Retained Roadways. Int. J. Rock. Mech. Min. Sci. **134**, 104436 (2020). DOI: https://doi.org/10.1016/j.ijrmms.2020.104436

[39] H.M. Westergaard, Theory of Elasticity and Plasticity American Journal of Physics. Amer. J. Phys. **34**, 545 (1966). DOI: https://doi.org/10.1119/1.1973102

[40] X.X. Miao, X.B. Mao, G.W. Hu, Research on Broken Expand and Press Solid Characteristics of Rocks and Coals. J. Exp. Mech. **12**, 394-400 (1997).

[41] M.C. He, Y.B. Gao, J. Yang, W.L. Gong, An Innovative Approach for Gob-Side Entry Retaining in Thick Coal Seam Longwall Mining. Energies **10** (11), 1785 (2017). DOI: https://doi.org/10.3390/en10111785

[42] T. Janoszek, The Assessment of Longwall Working Stability Based on the Mohr-Coulomb Stress Criterion – Numerical Analysis. Arch. Min. Sci. **65** (2), 493-509 (2020). DOI: https://doi.org/10.24425/ams.2020.134131

[43] L. Herezy, D. Janik, K. Skrzypkowski. Powered Roof Support – Rock Strata Interactions on the Example of an Automated Coal Plough System. Stdu Geotrch Mech. **40** (1), 46-55 (2018). DOI: https://doi.org/10.2478/sgem-2018-0007

[44] S. Rajwa, The Influence of the Geometrical Construction of the Powered Roof Support on the Loss of a Longwall Working Stability Based on the Practical Experience. Arch. Min. Sci. **65** (3), 511-529 (2020). DOI: https://doi.org/10.24425/ams.2020.134132